Study on the Train-Induced Vibration Transmission Within the Over-Track Building

Lihui Xu, Xiaojing Sun and Rongning Cao

Abstract The integrated complexes, known as the over-track building and metro depot complexes, have been widely developed in recent years in China. The construction of the over-track buildings has great merits of reductions in occupying urban land, conveniences in commuting to work, and comprehensive exploitation of the upper spaces. Such complexes have some negative effects that the train operation into and out of the depots can induce structural vibrations causing discomfort on occupants inside the buildings. To characterize the vibration transmissions between the floors, the three-dimensional dynamic finite element model of soil-platform-building has been established. The coupled train–track model was studied and applied as well in this paper. Diverse analyses of vibration responses have been conducted including vibration acceleration levels and vibration acceleration spectra in frequency domain and in 1/3 octave frequency. It found that vibration transmission law across floors in the horizontal orientation inside the over-track building absolutely differs from that in the vertical orientation. Train-induced vibrations inside the over-track building are mainly distributed in high frequency within 30–80 Hz, which have potential to make impacts on the occupants. Dynamic responses have revealed the key insights into the vibration transmissions in different orientations inside the over-track buildings.

Keywords Metro depot · Over-track building · Vibration · Numerical simulation · Vibration acceleration level · Frequency domain · 1/3 octave spectrum

L. Xu · X. Sun (✉) · R. Cao
Beijing Jiaotong University, Beijing 100044, China
e-mail: xjsun1@bjtu.edu.cn

L. Xu
e-mail: 17121129@bjtu.edu.cn

1   Introduction

Urban rail transit has great advantages in reducing the highway traffic in metropolitan city. For urban rail transit, subways have been widely developed due to its characteristics of efficient operation and less occupation of the ground areas. By the end of December 2017, in-service subway lines have spread over 34 cities with a total of 3884 km in mainland China [1]. The train depots are the subway or railway facilities for the regular maintenance, examination, and storage for the trains and usually occupy the large ground areas [2]. Traditional metro depots with low density of buildings hold larger ground spaces which make significant influences on the space and the environment, and it's not conducive to efficient utilization of the urban land and space due to the low density of the buildings [3]. Comprehensive utilization of the spaces above the depots can not only improve the utilization efficiency of the urban land, but also have great economic advantages. So, many cities in mainland China like Beijing and Wuhan have begun developing the over-track building complexes, which are built with a new structural system with large platforms, for residents and workers above the metro depot. The platforms above the metro depot are used for entertaining and parking, supported by the columns which are set in between train tracks.

However, the subway operation into and out of depots can generate excessive vibrations due to interaction between rails and wheels, which propagate from the tracks directly into the over-track buildings through ballast, columns, and platforms, radiating noises within the buildings that adversely affect the living qualities and even the health of the building occupants. It is essential to predict the train-induced vibration level prior to construction within the over-track buildings and take appropriate measures to mitigate the vibration for human comfort.

Massive researches have been conducted to characterize the vibration at the sources, in the propagation paths, and in the receivers inside the buildings induced by subway trains and operation lines. The vibration characteristics at the sources and in the propagation paths induced by railways have been summarized in detail [4–8]. Anderson [9] conducted measurements to collect the vibration data from two buildings caused by the railway operation and got that the perceptible vibrations, which are mainly between 5 and 50 Hz, can transmit into the building through the ground. Xia et al. [10] took in situ experiment to examine the vibration levels induced by running trains near Shenyang–Harbin railway line within two buildings and found the acceleration levels in the buildings exceeded the allowance by the Chinese Code. Sanayei et al. [11, 12] performed measurements of train-induced and subway-induced vibrations in different areas in Boston. It provided the basis that the vibration levels in sensitive locations inside the buildings induced by train operations should be estimated precisely. Numerous prediction modeling methods have been developed to predict the subway-induced vibration from the underground lines [13–16].

The vibration transmission in metro depots entirely differs from that around the operation line and subways, for the trains work on the ground right under the platform and the over-track buildings which is not the case with the operation lines and

subways. Some studies have been conducted on the transmission characteristics and levels of the vibration on the grounds, platforms, and over-track buildings in the metro depots. Field measurements were conducted to study the law of the vibration attenuation in the ground, platforms, and the over-track buildings subject to the vibration input in throat area [17], in testing line area [18], and in both throat and testing line areas [2, 3]. The measured maximum vertical vibration levels were lower than the limitation by Chinese standard [19] according to these researches. Numerical models were established to analyze the vibration response of the over-track buildings [20–22]. Vibration data of the sources were measured in the time domain on site and applied into the established numerical model. The results from the numerical model were well consistent with the measured vibration in the over-track buildings in both time and frequency domain, and the models were used to predict the vibration levels prior to the construction of the over-track buildings. He et al. [23] studied the impact of the train speed on the vibration within the over-track buildings and concluded that limiting the train speed into and out of the metro depot is an efficient way to attenuate the vibration within the over-track buildings.

This passage is to study the characteristics of the vibration transmission inside the over-track building above the main body in a typical metro depot under the influence of subway operation. A three-dimensional dynamic finite element model of soil-platform-building was built according to a metro depot to characterize the vibration transmission, and the train-induced vibrations were compared with the limitation by Chinese standard. It is efficient and reliable to apply this model to predict the vibration levels in the over-track building before constructing.

## 2   Description of Metro Depot and Over-Track Building

The metro depot related to this study is situated in Beijing, China. Its total occupying land use is approximately 314,200 m^2, including 266,000 m^2 for the functions of metro depot and 48,200 m^2 for the exploitation, which makes the metro depot the biggest one in China. Two avenues are situated at the north and west of the metro depot, respectively, as shown in Fig. 1. The soil layers consist of artificial accumulation layer, recent sedimentary layer, new Quaternary alluvium, and late Quaternary Pleistocene flood alluvium below the ground in this area. There is a main body, a throat area, and so on in the metro depot, and the tracks in the main body are straight. The area above the metro depot preserved for the construction of the over-track buildings with 12 floors is about 150,000 m^2, which will serve for the occupants and workers.

All the buildings are constructed using reinforced concrete columns with large open spans from the ground to the platform, whose height is 16.3 m to guarantee enough space for the trains. The columns supporting the platform have the sectional dimensions of 1.2 m by 1.2 m and are located on a grid of 6.0 m × 6.0 m, which is the same case with the columns supporting the over-track buildings according to the plan. The support structures for over-track building from the first floor to the top consist of frame structures with 12 floors with the height of 5.6 m in the first floor
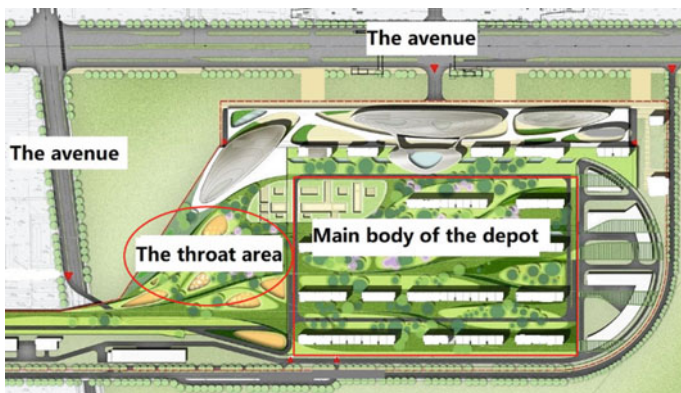
Fig. 1 Areas distribution in Beijing metro depot

Fig. 2 A sketch map of the metro depot in vertical direction
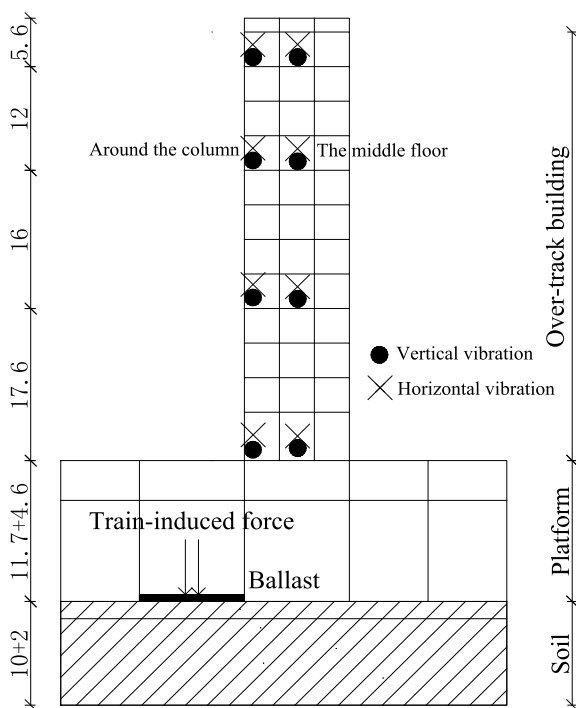
and the height of 4 m in standard floors, and load-bearing walls with the thick of 0.2 m, as shown in Fig. 2. The beams inside over-track building have the sectional size of 0.4 m × 0.6 m.

This study focused on vibration transmissions within an over-track building with 12 floors above the main body of the depot induced by the train operation into and out of the metro depot.

3 Establishment of the Finite Element Model

3.1 The Finite Element Model

As described above, the studied metro depot captures a large land use area. The vibration induced by the subway operation attenuates quickly with the propagation of the vibration wave, which makes it unnecessary to take all areas of metro depot into account in the study. A part of metro depot is applied in this model that must take a reasonable size for the reasons that a model which is too large can increase the computational cost and which is too small can affect the accuracy and reliability of the results [24]. The lengths of this model which are parallel to the track lines are 96 m and the widths which are perpendicular to the track lines are 51 m to make sure it is accurate and reliable to predict the vibrations. The height of the platform is 16.3 m to provide enough space for the trains.

The structure modeling and dynamic analysis are accomplished in the finite element software, ANSYS, which is widely used for modeling and analysis in statics and dynamics. The finite element model is shown in Fig. 3, and Fig. 2 shows the positions of train-induced forces which is a function of time acting at the point where fasteners and sleepers contact with each other. The points where the vertical and horizontal vibration data is gathered inside the over-track buildings, including the points on the floors around the column and the points in the middle of floors, are also illustrated in Fig. 2. In this model, all the beams and columns with different sectional size are simulated by the beam elements, BEAM4, which do not allow for shear deformations of the units. All the floors and walls are modeled using the surface elements, PLANE42, and soil and ballasts are regarded as the physical

Fig. 3 Finite element model of metro depot
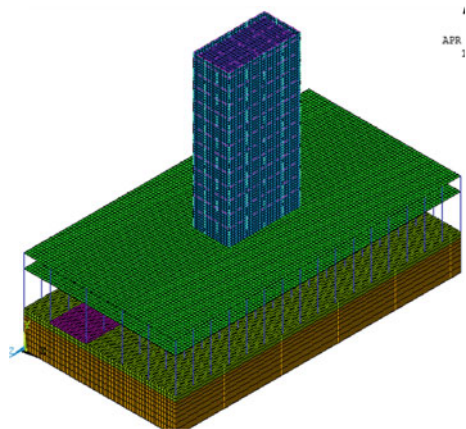
elements, SOLID45. The elements should be divided into small elements with the right sizes, which should be small enough to accurately determine the full waveform when vibration waves are propagating in the units and big enough to reduce the calculation time [24]. For the purpose of impeding wave reflection in the cut-off boundaries which are employed to take constraints to models from the infinite stratum into consideration, the viscoelastic boundaries are applied with the advantages of good behaviors in numerical stability and accuracy and its convenience of application in the finite element models [25].

Impacts of ballast, formation, building foundations, frame structures, and wall panels on the wave propagation in the depot are taken into account, and the effects of decorative components such as wall materials are ignored in this three-dimensional finite element dynamic model.

3.2 Damping

Damping is a so complicated mechanism of energy dissipation that many damping models have been put forward to make it easy to consider it in the researches and the Rayleigh damping model with a linear combination of stiffness and mass matrix is widely used. In order to determine the damping coefficients, the modal analysis is required to obtain the natural frequency of the building, and the first five levels of modal frequencies obtained from the modal analysis of the soil-platform-structure model are 1.00, 1.36, 2.40, 3.47, and 5.48 Hz, respectively. The mass damping coefficient and stiffness damping coefficient are acquired by taking the first two natural frequencies and damping ratios into Eq. (1).

$$
\begin{cases}
\alpha = \dfrac{4\pi f_i f_j \left(\varepsilon_j f_i - \varepsilon_i f_j \right)}{f_i^2 - f_j^2} \\[4mm]
\beta = \dfrac{\left(\varepsilon_i f_i - \varepsilon_j f_j \right)}{\pi \left(f_i^2 - f_j^2 \right)}
\end{cases}
\tag{1}
$$

where α and β are mass and stiffness damping coefficient, f_i, f_j, ε_i, ε_j are the ith and jth natural frequencies and damping ratios, which are 1.0 Hz, 1.36 Hz, 0.03, and 0.03 when i equals to 1 and j equals to 2, respectively. The value of α and β on the basis of Eq. (1) are 0.217 and 4.04×10^{-3}.

4 Vibration Sources

Simulation of train-induced excitation at the sources is one of the key processes in this study on the train-induced vibration transmission within the over-track building, because whether the input excitation is well consistent with the measured

excitation directly make impacts on correctness of the results. The method to cal-culate the excitation in frequency domain with coupled train–track dynamic model presented by Ma [26, 27], which has been confirmed by a number of field mea-surements, is studied and applied in this work.

4.1 The Coupled Train–Track Model

In the coupled train–track system, the trains which can move forward at the speed of v on the rails consist of several individual vehicles, and each vehicle is made up of three parts including a body, two bogies, and four wheelsets that each part connects to the others with parallel springs and dampers, as shown in Figs. 4 and 5. There are 10 degrees of freedom for a single vehicle, including ups and downs of the body, two bogies, and four wheelsets, as well as rotations about the axial direction of the body and two bogies. The suspended mass and the interactions between wheels and rails are also taken into account in this model. The interactions across the interfaces between rails and sleepers are nonlinear that are represented by a series of springs and dampers, which is the same case with sleepers and ballasts, as well as ballasts and foundations.

In vehicle model, there are 10 degrees of freedom for a certain vehicle, and the equation of motion in different degree of freedom should be formed to obtain the dynamic response. The equation of motion is shown as Eq. (2), on the basis of D'Alembert principle.
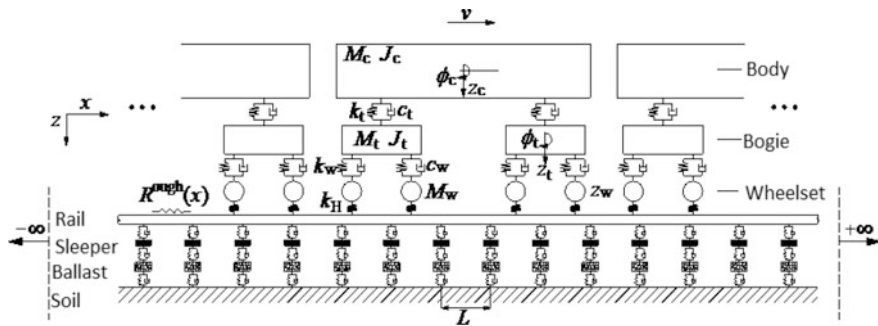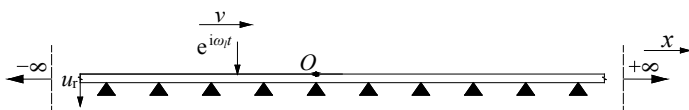

Fig. 4 Coupled train–track model

Fig. 5 Basic cell in global coordinate system

$$\mathbf{M}_m\ddot{\mathbf{A}}_m(t) + \mathbf{C}_m\dot{\mathbf{A}}_m(t) + \mathbf{K}_m\mathbf{A}_m(t) = \mathbf{Q}_m(t) \tag{2}$$

where $\ddot{\mathbf{A}}_m(t), \dot{\mathbf{A}}_m(t), \mathbf{A}_m(t)$ are the acceleration, velocity, and displacement vector of the certain vehicle, $\mathbf{Q}_m(t)$ are the excitation vector and $\mathbf{M}_m$, $\mathbf{C}_m$, and $\mathbf{K}_m$ are the mass, damping, and stiffness matrix.

Rails in this model are simplified as the Euler–Bernoulli beams ignoring the shear deformations across the transverse sections, which are infinite in the space and periodically supported by the vertical springs and dampers. The dynamic displacement of the infinite beam can be written as Eq. (3).

$$E_r^* I_r \frac{\partial^4 u_r}{\partial x^4} + m\frac{\partial^2 u_r}{\partial t^2} = e^{i\omega_l t}\delta(x - x_0^F - vt) - \sum_{n=-\infty}^{n=+\infty} f_n(t)\delta(x - x_n) \tag{3}$$

where u_r represents the vertical displacement, $E_r^* = E_r(1 + i\eta_r)$ are the elastic modulus which allows for the real elastic modulus E_r and the damping loss factor η_r. I_r and m are the sectional moment of inertia and mass per unit length, respectively. x_0^F is the location of the load at the initial time, and $x_n = nL$ is the location of the nth fastener where L represents the spacing between the adjacent fasteners. $f_n(t)$ is the support force from the nth fastener.

Solution of dynamic responses of the infinite beams can be carried out in a basic cell with the length of L, and the operations are conducted in global coordinate system in frequency domain, as shown in Fig. 5 and expressed as Eq. (4).

$$E_r^* I_r \frac{\partial^4 u_r}{\partial x^4} + m\frac{\partial^2 u_r}{\partial t^2} = e^{i\omega_l t}\delta(x - x_0^F - vt) \tag{4}$$

Fourier transformation is used to transform Eq. (4) from the time domain to the frequency domain, expressed as Eq. (5)

$$E_r^* I_r \frac{d^4 \hat{u}_r}{dx^4} - \omega^2 m\hat{u}_r = \frac{1}{v}e^{i\frac{\omega_l - \omega}{v}\left(x - x_0^F\right)} \tag{5}$$

where the $\hat{u}_r$ is the vertical displacement of the basic cell in frequency domain.

The displacements of a fixed point in the basic cell due to the unit harmonic moving load acting at the beams can be calculated using the method proposed by Ma [26, 27], and displacements of the points in other ranges are derived from solutions of the basic cell, which must comply with the periodic-infinite structure theory, expressed as Eq. (6).

$$\hat{u}_r(\widehat{x}, \omega, \omega_l) = e^{i(\omega_l - \omega)n_L L/v} \cdot \hat{u}_r(x, \omega, \omega_l) \tag{6}$$

where $\widehat{x}$ and x obey the relation of $\widehat{x} = x + n_L L$, L represents the length of basic cells, n_L refers to the number of the basic cells between the point at $\widehat{x}$ and x, and $\widehat{u}_r(x, \omega, \omega_l)$ is the displacement of the basic cell in frequency domain.

Continuous discrete displacements of points in whole beams induced by the unit harmonic moving load $F(t) = e^{i\omega_l t}$ at the speed of v are obtained through making the angular frequency ω continuous discrete values at the focused range in frequency domain. Then, applying the inverse discrete Fourier transformation, the displacements in frequency domain can be transformed to the displacements in time domain.

Train's passage would generate dozens of moving loads with certain magnitude, and all of them make contribution to the total displacements of the targeted point that are the linear superposition of influence under the individual one. The actual forces interacting across interfaces between rails and foundation are products of the actual displacements and composite stiffness allowing for the stiffness between the rails and sleepers, sleepers and ballasts, as well as the ballasts and foundation.

4.2 Excitation Due to Moving Trains

This work is based on operation of the Type-B train at the speed of 25 km/h which is integrated by six single vehicles. The vehicle parameters and track parameters are listed in Tables 1 and 2. The simulated excitation is illustrated as Fig. 6. The maximum of interacting forces between the rails and foundation induced by train operations are approximately 6×10^4 N, and the forces are mainly in low frequency within 10 Hz. The force magnitude in high frequency is low.

Table 1 Vehicle parameters

Parameter's name		Values
Body parameters	Vertical stiffness	480 kN/m
	Vertical damping	60 kN s/m
	Mass of an individual vehicle	43 t
Bogies parameters	Vertical stiffness	1650 kN/m
	Vertical damping	15 kN s/m
	Mass of a single bogies	3.418 t
Wheelsets parameters	Mass of an single wheel	1.61 t
	Radius of the wheels	0.84 m
	Spacing between wheels in one bogie	2.2 m

Table 2 Track parameters

Parameter's name		Values
Steel rail parameter	Mass per unit length	$m = 121.28 \, \text{kg/m}$
	Elastic modulus	$E_r = 2.059 \times 10^{11} \, \text{N/m}^2$
	Moment of the inertia across the section	$I_r = 6.434 \times 10^{-5} \, \text{m}^4$
	Damping loss factor	$\eta_r = 0.01$
Fastener parameter	Stiffness	$k_r = 1.2 \times 10^8 \, \text{N/m}$
	Damping	$c_r = 6 \times 10^4 \, \text{N s/m}$
	Spacing between adjacent fasteners	$L = 0.6 \, \text{m}$
Ballast parameter	Density	$\rho_b = 1.8 \times 10^3 \, \text{kg/m}^3$
	Elastic modulus	$E_b = 1.1 \times 10^8 \, \text{N/m}^2$
	Damping	$c_b = 5.88 \times 10^4 \, \text{N s/m}$

(a) Force in time domain   (b) Force in frequency domain
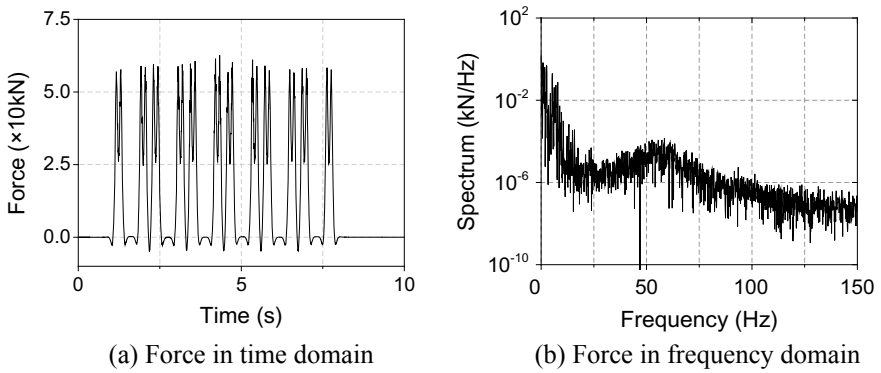
Fig. 6 Train-induced interacting force between rails and foundation

5 Train-Induced Vibrations Inside the Over-Track Building

In order to characterize the vibration transmissions inside the over-track building subjected to the train operation, points for gathering vertical and horizontal vibration data are appointed to be located at each floor around the column and in the middle of each floor, as illustrated in Fig. 2. The analyses of vibration responses are conducted in three aspects including vibration acceleration levels, vibration acceleration spectra in frequency domain, and in 1/3 octave frequency. According to ISO 2631-1 [28], the main frequencies of vibration impacts on humans are within 1–80 Hz. As a result, frequencies in this study range from 1 to 100 Hz.

5.1 Vibration Acceleration Level

The vibration acceleration levels are used for evaluating impacts of vibrations inside buildings, which are induced by the vibration sources within the buildings, such as elevators, motors, and so on, formulated by GB/T 50355-2005 [29]. The method of calculating the vibration acceleration level has been made by it, expressed as Eq. (7).

$$L_a = 20 \lg \frac{a_{rms}}{a_0} \qquad (7)$$

where a_0 is the reference acceleration with the value of 1×10^{-6} m/s^2, a_{rms} is the root mean square of acceleration value (m/s^2), and L_a represents the vibration acceleration level (dB).

Figure 7 shows vertical vibration acceleration levels around the column and in the middle of the floor inside the building. The vertical vibration acceleration levels are attenuated between the first to the ninth floor around the column and the first to tenth floor in the middle of floors and amplified greatly at the top floor, with the minimum of approximately 46.2 and 52.6 dB, respectively. What is more, the vertical vibration acceleration level around the column is less than that in the middle of the floor by 1.8–6.9 dB in the same floor. Vertical constraint from the column makes the floor vibration weaker around the column, and vibration waves from various propagation paths strengthen each other in amplitude in the middle of floors, which may contribute to that phenomenon.

The horizontal vibration acceleration levels around the column and in the middle of the floor inside the building are shown in Fig. 8. The horizontal vibration acceleration levels around the column and in the middle of the floor in the same height are comparably close, with little differences in magnitude. The horizontal vibration levels show the tendency of slight amplification on the whole, with no

Fig. 7 Vertical acceleration level inside the building
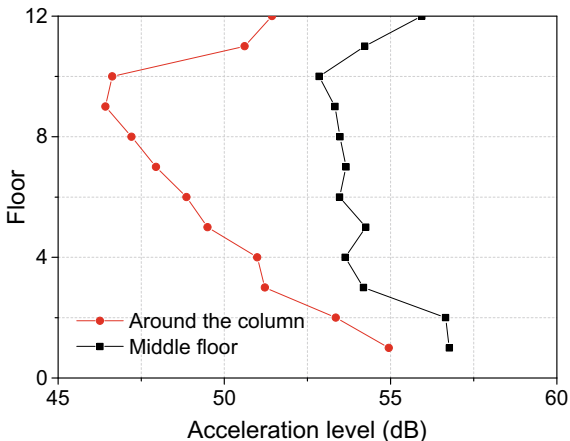
**Fig. 8** Horizontal acceleration level inside the building
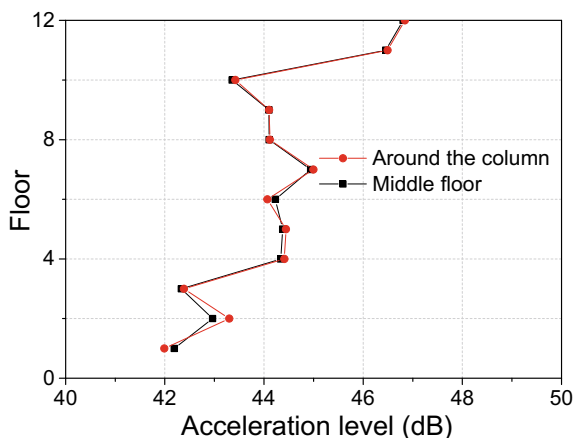
attenuation, with the increase in height, which can be explained by the cause that the floors are more weakly restrained in the horizontal direction in higher floors.

Comparing Figs. 7 and 8, it is evident that the vibration acceleration levels in vertical orientation are greater than those in horizontal orientation by 7.8–14.6 dB in the same floor. This is because the moving loads induced by the train operation in the straight track are mainly vertical and stiffness in vertical direction are smaller than that in horizontal direction in the middle of the floor that vibrations are amplified with the stiffness degradation.

5.2 Spectrum in Frequency Domain

Figures 9, 10, and 11 typically show a portion of vibration acceleration spectra in frequency domain both around the column and in the middle of the floors. In both vertical and horizontal directions, the train-induced vibrations inside the building are mainly distributed in high frequency within 30–80 Hz, which could make impacts on the occupants, and the dominant frequency decreases with the rise in height. As shown in Figs. 9 and 10, the dominant frequencies of vertical vibrations in the middle of the floors are basically consistent with these on the same floor around the column, which range from 50 to 70 Hz. Moreover, the dominant frequencies of the floor vibrations in horizontal direction, varying between 30 and 55 Hz, are lower in comparison with these in vertical direction by about 15 Hz, as shown in Fig. 11. Also, the maximums of the horizontal vibration amplitudes are obviously below these in vertical direction.

There exist the regularities that the vibrations inside the over-track building are enhanced at certain frequencies, which are near 23, 35, 75 Hz. That is because the train-induced vibrations within the building have triggered the certain bending mode of the floor slabs, whose frequencies are exactly corresponding to these where
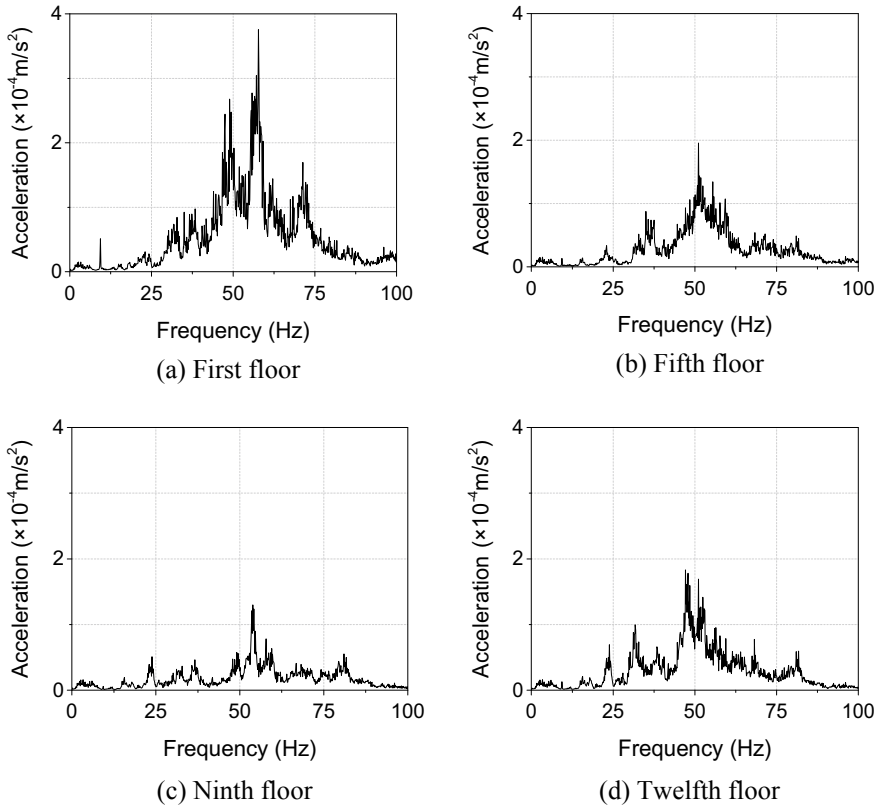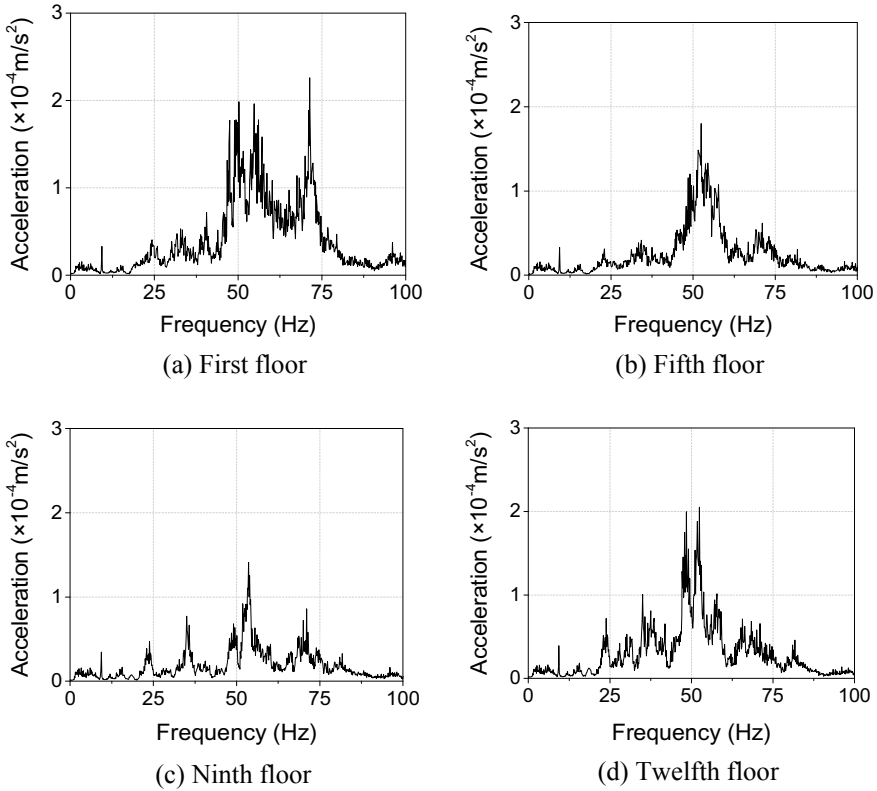
Fig. 9 Train-induced vertical vibrations in the middle of the floors

the vibrations are largely amplified. Additionally, it is quite clear from the graphic area enclosed by the curves of the vibration acceleration spectra and the transverse axis that the horizontal vibration energy, which is mostly distributed at some specific frequencies, is more concentrated than the vertical vibrations in frequency domain.
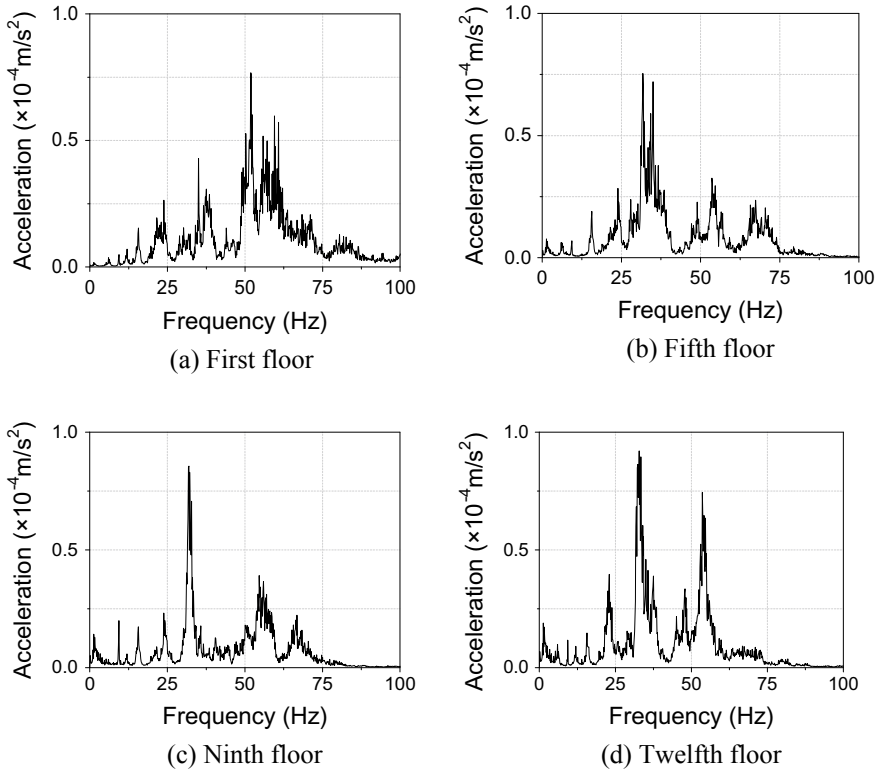
5.3   1/3 Octave Spectrum

The vertical vibration acceleration spectra in 1/3 octave frequency on the floors around the column and in the middle of the floors are shown in Figs. 12 and 13. It can be obviously found that when the central frequency is below 10 Hz, the vertical acceleration levels of each floor are approximately equivalent, with the differences below 5 dB. The vertical vibrations attenuate slowly in the low frequency during the transmission between floors. When beyond 16 Hz, the acceleration levels

(a) First floor

(b) Fifth floor

(c) Ninth floor

(d) Twelfth floor

**Fig. 10** Train-induced vertical vibrations around the column

change quickly with the rise in height. It also can be noticed that the vertical acceleration level reaches a peak value at 16 Hz and the maximum at 63 Hz. Then above 63 Hz, the acceleration levels fall off rapidly. Comparing to allowance by the standard of limit and measurement method of vibration in the room of residential buildings [29], the vertical acceleration levels inside the over-track building are far below the limitation.

Figure 14 shows the 1/3 octave spectra of the horizontal vibration acceleration levels in the middle of the floors. The horizontal vibration levels increase monotonously and greatly with the rise in height, in which the vibration level in the first floor is lower than that in the top floor by about 20 dB, when the central frequency is smaller than 6.3 Hz. Inversely, when above that, the vibration levels change slowly and the differences are not that great between different floors. Meanwhile, the horizontal vibration levels are of little changes in the low frequency, and these are in sharp variations when the central frequency goes beyond 6.3 Hz. And the acceleration levels in horizontal direction reach the maximum at the 31.5 Hz.

(a) First floor
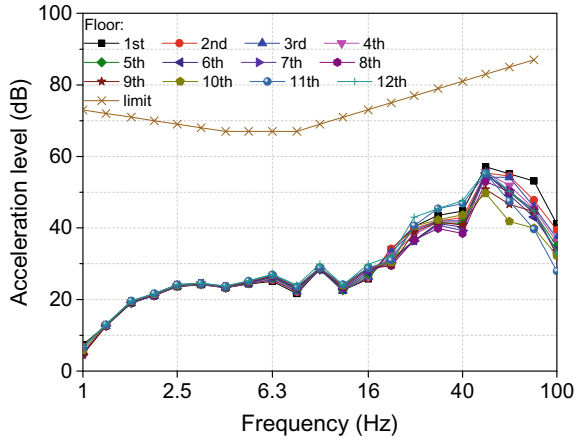
(b) Fifth floor

(c) Ninth floor

(d) Twelfth floor

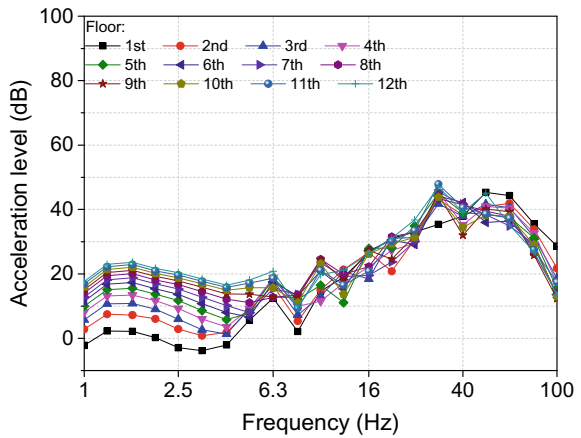**Fig. 11** Train-induced horizontal vibrations in the middle of the floors

Fig. 12 1/3 octave spectra of the vertical vibrations in the middle of the floors
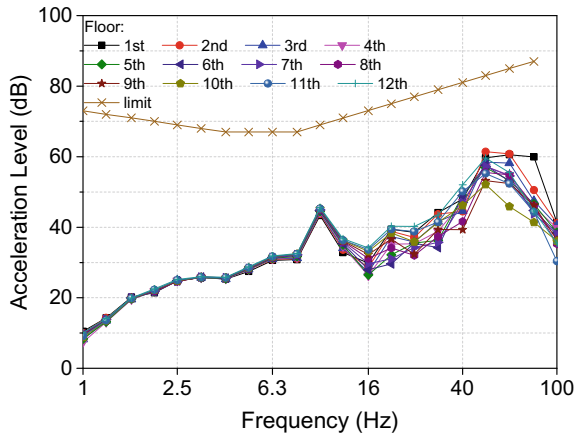
Fig. 13 1/3 octave spectra of
the vertical vibrations around
the column

Fig. 14 1/3 octave spectra of
the horizontal vibrations in
the middle of the floors

It can be inferred from the analyses above that the vibration transmission law
across the floors in the horizontal orientation inside the over-track building abso-
lutely differs from that in the vertical orientation. What is more, there are some
diversities between the distribution of the horizontal vibration 1/3 octave spectra in
the first floor of the building and that in standard floor in high frequency, whose
heights are 5.6 and 4 m, respectively. This is because the horizontal constraints to
the first floor are imposed by the platform, which could make it vibrate in a different
way.

6   Conclusion

Three-dimensional dynamic finite element model of soil-platform-building was established to characterize the vibration transmissions inside the over-track building induced by the train operations into and out of the metro depot. The coupled train–track model was studied and applied as well. These findings have revealed the key insights into the vibration transmissions inside the over-track buildings, including:

1. Vibration waves from various propagation paths strengthen each other in amplitude in the middle of floors, which results in amplifying the vertical vibrations by more than 1.8 dB in comparison with the vertical vibration levels around the columns inside the building. The horizontal vibration levels are comparable in the same floor.
2. The weaker constraints to the higher floors in horizontal direction make main contributions to the vibration enhancement that makes horizontal vibration levels with the tendency of amplification on the whole with the rise in height. The vertical vibrations are attenuated by the floors and amplified at the top floor.
3. Train-induced vibrations inside the over-track building are mainly distributed in high frequency within 30–80 Hz, which have potential to make impacts on the occupants, and the dominant frequency decreases with the rise in height in both vertical and horizontal direction.
4. In the 1/3 octave frequency, the vertical vibration acceleration levels in high frequencies change more obviously with the increasing floor, and the horizontal vibration acceleration levels in low frequencies change more obviously with the increasing floor.

References

1. Urban Rail Transit Association (2017) Annual statistics and analysis report of urban rail transit of 2017—the 2nd version. http://www.camet.org.cn. Accessed 2018/04/08
2. Zou C, Wang YM, Wang P et al (2015) Measurement of ground and nearby building vibration and noise induced by trains in a metro depot. Sci Total Environ 536:761–773
3. Zou C, Wang YM, Moore JA et al (2017) Train-induced field vibration measurements of ground and over-track buildings. Sci Total Environ 575:1339–1351
4. Connolly DP, Kouroussis G, Laghrouche O, Ho CL, Forde MC (2015) Benchmarking railway vibrations-track, vehicle, ground and building effects. Constr Build Mater 92:64–81
5. Kouroussis G, Connolly DP, Verlinden O (2014) Railway-induced ground vibrations–a review of vehicle effects. Int J Rail Transp 2(2):69–110
6. Hung H, Yang Y (2000) A review of researches on ground-borne vibrations with emphasis on those induced by trains. Proc Nat Sci Counc Part A Phys Sci Eng 25(1):1–16
7. Newland DE, Hunt HEM (1991) Isolation of buildings from ground vibration: a review of recent progress. Proc Inst Mech Eng Part C Mech Eng Sci 205(1):39–52
8. Avillez J, Frost M, Cawser S, Skinner C, El-Hamalawi A, Shields P (2012) Procedures for estimating environmental impact from railway induced vibration: a review. In: ASME 2012

noise control and acoustics division conference at InterNoise 2012, Aug 2012. American Society of Mechanical Engineers, pp 381–392

9. Anderson DC (1994) Engineering prediction of railway vibration transmitted in buildings. Environ Eng 7(1):14–19

10. Xia H, Zhang N, Cao YM (2005) Experimental study of train-induced vibrations of environments and buildings. J Sound Vib 280(3–5):1017–1029

11. Sanayei M, Maurya P, Moore JA (2013) Measurement of building foundation and ground-borne vibrations due to surface trains and subways. Eng Struct 53:102–111

12. Sanayei M, Moore JA, Brett CR (2014) Measurement and prediction of train-induced vibrations in a full-scale building. Eng Struct 77:119–128

13. Gupta S, Hussein MFM, Degrande G, Hunt HEM, Clouteau D (2007) A comparison of two numerical models for the prediction of vibrations from underground railway traffic. Soil Dyn Earthq Eng 27(7):608–624

14. Hussein MFM, Hunt HEM (2009) A numerical model for calculating vibration due to a harmonic moving load on a floating-slab track with discontinuous slabs in an underground railway tunnel. J Sound Vib 321(1–2):363–374

15. Thornely-Taylor RM (2004) The prediction of vibration, ground-borne and structure-radiated noise from railways using finite difference method—part 1—theory. Proc Inst Acoust 26(Pt 2):69–79

16. Jones S (2010) Ground vibration from underground railways: how simplifying assumptions limit prediction accuracy. Ph.D. thesis, University of Cambridge, Cambridge

17. Zou C, Wang YM, Wang ZH et al (2015) Field measurement and analysis of ground vibration in the throat area of metro depot. J Vib Shock 34(16):200–206

18. Lin CJ, Qi YK, Xing Y et al (2015) Propagation law of vibration from test line in metro depot. Urban Rapid Rail Transit 28(05):77–81

19. Ministry of Environment Protection of the People's Republic of China (1988) GB 10070-88: standard of vibration in urban area environment

20. Li XL (2003) Study on influence of vibration induced by subway train on ground and ground structures. Ph.D. thesis, Beijing University of Technology, Beijing

21. Wu YB, Zhang B, Liu YH et al (2015) Law of vibrations influence of subway on metro depot superstructure. J China Railw Soc 37(08):98–103

22. Xie WP, Chen YM, Yao CQ (2016) Vibration analysis of train depot over-track buildings induced by train load. J Vib Shock 35(08):110–115

23. He L, Song RX, Wu YB et al (2015) Analysis on actual measurement of train speed influence on the vibration of over-track buildings of metro depot. Build Struct 45(19):96–99

24. Liu WN, Ma M et al (2014) Prediction, evaluation and control of the environmental vibration induced by subway trains. Science Press, Beijing

25. Gu Y, Liu JB, Du YX (2007) 3D consistent viscous-spring artificial boundary and viscous-spring boundary element. Eng Mech 24(12):31–37

26. Ma LX (2015) Study on the model of coupled vehicle and track and the analysis model for tunnel-ground vibration response based on the periodic-infinite structure theory. Ph.D. thesis, Beijing Jiaotong University, Beijing

27. Ma LX, Liu WN, Li KF (2014) Fast numerical algorithm of floating slab track vibration response under moving loads in the frequency domain. J China Railw Soc 36(02):86–94

28. International Organization for Standardization (1997) ISO 2631-1: mechanical vibration and shock—evaluation of human exposure to whole-body vibration—part 1: general requirements

29. Ministry of Construction of the People's Republic of China (2005) GB/T 50355-2005: standard of limit and measurement method of vibration in the room of residential buildings